PHYSICAL REVIEW B VOLUME 38, NUMBER 15 15 NOVEMBER 1988-II

Anisotropy of the third-order nonlinear-optical susceptibility in a degenerate-ground-state conjugated polymer: *trans*-$(\mathrm{CH})_x$

M. Sinclair, D. Moses, K. Akagi,* and A. J. Heeger†
Department of Physics and Institute for Polymers and Organic Solids, University of California, Santa Barbara, California 93106

(Received 14 December 1987)

We present the results of a series of third-harmonic-generation (THG) measurements on the conjugated polymer polyacetylene which probe the magnitude and the origin of the third-order nonlinear-optical susceptibility of this material. By performing reflection THG measurements relative to a silicon standard, we have unambiguously determined the magnitude of the third-order susceptibility associated with tripling the fundamental of the Nd:YAG laser to be $\chi_{\parallel}^{(3)}(3\omega;\omega,\omega,\omega)=(4\pm2)\times10^{-10}$ esu, where $\chi_{\parallel}^{(3)}$ refers to that component of the third-order susceptibility tensor with all indices parallel to the chain direction. By measuring anisotropic THG in oriented films, we have shown that this component dominates. The magntiude and anisotropy are directly compared with results obtained from single crystals of polydiacetylene-(toluene-sulfonate) measured in the same apparatus. Finally, we have measured THG in both *cis*-rich and *trans* isomers of the same sample. We found that the measured response of the *cis*-rich samples scales with the residual *trans* content of the sample; $\chi_{\parallel}^{(3)}$ of the *trans* isomer is 15–20 times larger than that of the *cis* isomer. This symmetry-specific aspect of $\chi^{(3)}$ implies a mechanism which is sensitive to the existence of a degenerate ground state, as in *trans*-$(\mathrm{CH})_x$; it is consistent with the virtual generation of nonlinear solitons as a mechanism for the large measured third-order nonlinear-optical susceptibility of polyacetylene.

I. INTRODUCTION

Although organic polymers have great potential for eventual application in nonlinear-optical elements, an understanding of the mechanism (or mechanisms) underlying their nonlinear susceptibilities is necessary before the design and synthesis flexibility afforded by organic chemistry can be applied to the development of new and better materials. Detailed experimental studies of prototype systems must therefore be performed in order to guide a parallel theory effort aimed at a general understanding of the nonlinear-optical properties of organic polymer materials.

The promise of conducting polymers as fast-response nonlinear-optical materials has been recently emphasized.[1–3] Polymers such as polyacetylene, polythiophene, and the soluble and processible poly(3-alkylthienylenes) contain a high density of π electrons, and they are known to exhibit photoinduced absorption and photoinduced bleaching, indicating major shifts of oscillator strength upon photoexcitation.[2,4] For polyacetylene, these nonlinear effects have been studied in detail in the picosecond[5(a),5(b)] and subpicosecond[5(c)] time regimes and have been correlated with the photoproduction of charge carriers through fast-photoconductivity measurements.[6] The data have demonstrated ultrafast response with nonlinear shifts in oscillator strength occurring at times of the order of 10^{-13} s. These *resonant* nonlinear-optical properties are intrinsic; they originate from the nonlinearity of the self-localized photoexcitations[7] which characterize this class of polymers: solitons, polarons, and bipolarons.[4]

In any material where photoexcitation results in shifts of oscillator strength (as is the case in conducting polymers), the optical properties will be highly nonlinear. The magnitude of the *resonant* $\chi^{(3)}$ can be estimated from the magnitude and frequency dependence of the photoinduced absorption and bleaching. For example, as a result of the shift in oscillator strength subsequent to photoexcitation, the complex index of refraction is intensity dependent,

$$n(\omega)=n_0(\omega)+n_2(\omega,\omega_p)I(\omega_p)\ , \tag{1}$$

where the second term describes the nonlinear response at frequency ω due to an intense pump at pump frequency ω_p. Under pumping conditions which are resonant with the π-π^* transition of polyacetylene ($\hbar\omega_p=2.0$ eV), the existing data yield an estimate[2,7] for n_2(1.4 eV, 2.0 eV) $\approx10^{-4}$ $(\mathrm{MW/cm^2})^{-1}$. This large value for Δn implies a correspondingly large value for $\mathrm{Im}\chi^{(3)}$ through the relation

$$n_2=4\pi^2/c\epsilon\chi^{(3)}\ , \tag{2}$$

where ϵ is the dielectric constant at the probe frequency (ω). Using the above value for n_2, we obtain $\mathrm{Im}\chi^{(3)}(-\omega_2=\omega_1-\omega_1-\omega_2)=5\times10^{-8}$ esu, an impressive value even under resonant conditions. From a Kramers-Kronig analysis of the photoinduced absorption data, one concludes that the real parts of n_2 and $\chi^{(3)}$ are correspondingly large. Based on these observations, experimental studies of third-harmonic generation in polyacetylene and related conducting polymers were initiated in order to explore directly the third-order susceptibility under nominally *nonresonant* conditions where the pump is well below the principal interband (π-π^*) transition.

In this paper we present the results of a series of third-harmonic-generation (THG) measurements which probe the magnitude and the origin of the third-order nonlinear-optical susceptibility of polyacetylene. By performing reflection THG measurements relative to a silicon standard, we have unambiguously determined the magnitude of the third-order susceptibility associated with tripling the fundamental of the Nd:YAG (YAG denotes yttrium aluminum garnet) laser to be $\chi_{\parallel}^{(3)}(3\omega;\omega,\omega,\omega)=(4\pm2)\times10^{-10}$ esu, where $\chi_{\parallel}^{(3)}$ indicates that component of the third-order susceptibility tensor with all indices parallel to the chain direction. We have successfully measured the anisotropic THG in oriented thin films and demonstrated that all the nonlinearity is associated with the π-electron polarizability along the conjugated chain. The magnitude and anisotropy are directly compared with the results obtained from single crystals of polydiacetylene-(toluene-sulfonate), PDA-TS, measured simultaneously and in the same apparatus. When pumping at 1.06 μm (1.17 eV), the third-harmonic power generated (on reflection) from a cleaved single crystal of PDA-TS is about a factor of 2 greater than that from an oriented film of *trans*-$(\mathrm{CH})_x$. Finally, we have measured THG in *cis*-rich and *trans* isomers of the same sample. The measured response of the *cis*-rich samples scales with the residual *trans* content of the sample; $\chi_{\parallel}^{(3)}$ of the *trans* isomer is 15–20 times larger than that of the *cis* isomer. This symmetry specific aspect of $\chi_{\parallel}^{(3)}$ implies an underlying mechanism which is sensitive to the existence of a degenerate ground state, as in *trans*-$(\mathrm{CH})_x$. The large $\chi^{(3)}$ (when pumped) subgap is therefore consistent with the virtual generation of nonlinear solitons as a mechanism for the nonlinear-optical susceptibility of polyacetylene. This mechanism is developed and discussed in detail; we conclude that the nonlinear zero-point fluctuations of the ground state lead to an important mechanism for nonlinear optics, particularly in polymers with a degenerate ground state.

II. EXPERIMENTAL METHODS

Since *trans*-$(\mathrm{CH})_x$ is strongly absorbing at the third harmonic (355 nm) of the Nd:YAG pump laser, the technique developed by Burns and Bloembergen[8] for measurement of third-harmonic generation in absorbing media is most applicable. This method relies on measurement of the backward-moving wave at 3ω radiated by the nonlinear polarization. When the sample thickness is large compared to the absorption depth at 3ω, the amplitude of the reflected signal is independent of the sample thickness, and, for the case where the fundamental wave is normally incident on a "thick" sample, the amplitude of the reflected third-harmonic wave amplitude (E_R) is given by

$$|E_R(3\omega)|^2=|\chi^{(3)}(3\omega)|^2F(n_0,N_1,N_3)|E_i(\omega)|^6\,, \tag{3}$$

where $E_i(\omega)$ is the incident field amplitude, n_0 is the refractive index of the medium from which the pump is incident, N_1 and N_3 are the complex indices of refraction at ω and 3ω, respectively, and

$$F(n_0,N_1,N_3)=\frac{1024\pi^2n_0^6}{|n_0+N_1|^6\,|n_0+N_3|^2\,|N_1+N_3|^2}\,. \tag{4}$$

The principal difficulty in determining $\chi^{(3)}$ from Eqs. (3) and (4) is that of determining $E_R(3\omega)$ and $E_i(\omega)$ accurately. This is overcome by measuring the third harmonic generated by the sample relative to that generated by a reference sample with known $\chi^{(3)}$. In this way, uncertainties associated with determining the pump intensity at the sample and absolute detector calibration are avoided. If P_s and P_r are the third-harmonic powers generated by the sample and the reference under identical conditions, then one can determine the unknown $\chi^{(3)}$ using the relation

$$\frac{P_s}{P_r}=\frac{|\chi s^{(3)}|^2F_s}{|\chi r^{(3)}|^2F_r} \tag{5}$$

for the ratio.

The experimental arrangement used to measure the third-harmonic intensity is shown in Fig. 1. It consists of a mode-locked Nd:YAG laser and fiber-grating pulse compressor which produce an 82-MHz train of pulses with an autocorrelation [full width at half maximum (FWHM)] of 4.5 ps and ~5 kW peak power. A half-wave plate and polarizing cube were used as a variable attenuator, and the beam was directed onto the sample by means of a dichroic filter which was chosen to have high reflectivity at $\lambda=1.06$ μm and high transmissivity at $\lambda=355$ nm. The fundamental beam was focused to a spot size of ~30 μm at the sample by a converging lens which also served to recollimate the reflected third harmonic. After recollimation, the third harmonic passes through the dichroic filter and the notch filter to reach

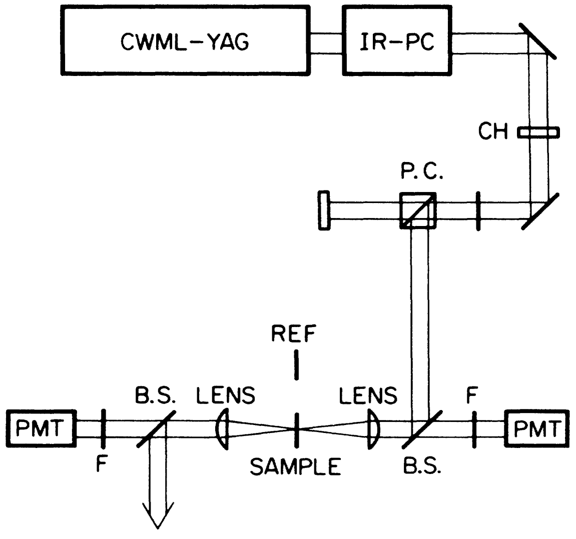

FIG. 1. Schematic diagram of the experimental arrangement used to measure the third-harmonic intensity.

the photomultiplier tube. A recollimating lens and dichroic filter were also mounted after the sample so that third-harmonic generation could also be measured in the transmission mode. The fundamental beam was chopped, and lock-in detection was used to measure the output of the photomultiplier tube. For the polarization-dependence measurements, an additional half-wave plate was inserted between the dichroic filter and the focusing lens to allow the polarization of the fundamental beam to be rotated at the sample.

The sample was attached to the cold finger of a Helitran cryostat; the vacuum shroud of the cryostat was mounted on an *XYZ* translation stage to facilitate focusing and to allow the samples to be moved in and out of the beam. A small piece of intrinsic silicon [cut with a (111) surface] was mounted immediately adjacent to the polymer sample to serve as reference. Relative measurements were taken by first measuring the third-harmonic signal reflected from the sample and then (without changing any of the parameters) translating the cryostat to measure the signal from the silicon reference.

The polyacetylene samples used in the anisotropy measurements were films of aligned *trans*-$(\mathrm{CH})_x$ grown on glass by the novel technique in which the catalyst for the polymerization reaction was suspended in a liquid-crystal solvent.[9,10] The polymerization reaction was carried out with the liquid-crystal (and catalyst) oriented in the ~ 1 T field of an electromagnet. Film thickness varied from $\sim 0.1\ \mu\mathrm{m}$ (for transmission measurements) to $\sim 1\ \mu\mathrm{m}$ (for reflection measurements). Studies of the anisotropy of the infrared absorption of polyacetylene samples prepared in this way[9] indicate that the polymer chains are aligned with a typical mosaic spread of $\approx \pm 15°-20°$. The comparative *cis-trans* measurements were carried out using nonoriented material prepared on glass substrates using the standard Shirakawa method. All reflection measurements were taken with the fundamental beam incident on the sample from the glass side ($n_0 = 1.5$) in order to take advantage of the superior surface quality on that side.

III. MAGNITUDE AND ANISOTROPY OF $\chi^{(3)}$ FOR *trans*-$(\mathrm{CH})_x$ AND FOR PDA-TS: A DIRECT COMPARISON

The third-harmonic power reflected from the (glass side) surface of the oriented *trans*-$(\mathrm{CH})_x$ samples (when the polarization of the fundamental beam is parallel to the alignment direction of the sample) is approximately 2000 times larger than the power reflected from the surface of intrinsic silicon under identical conditions. Assuming that the optical properties of the oriented samples are those determined for oriented Durham *trans*-polyacetylene,[11] the appropriate optical constants are as follows:

$$N_1 = (\epsilon_1)^{1/2} = 3.55 \quad \text{and} \quad N_3 = (\epsilon_3)^{1/2} = 5.55 + i3.04\ ,$$

$$N_1 = (\epsilon_1)^{1/2} = 3.8 \quad \text{and} \quad N_3 = (\epsilon_3)^{1/2} = 0.7 + i1.4\ ,$$

for silicon[12] and *trans*-$(\mathrm{CH})_x$ (Ref. 13), respectively. Using these values and Eq. (4) yields $F_{(\mathrm{CH})_x} = 3.4 \times 10^{-2}$ for *trans*-$(\mathrm{CH})_x$ and $F_{\mathrm{Si}} = 2.4 \times 10^{-4}$ for Si. Finally, with the help of Eq. (5) we calculate

$$\chi^{(3)} = (P_{(\mathrm{CH})_x}/P_{\mathrm{Si}})^{1/2}(F_{\mathrm{Si}}/F_{(\mathrm{CH})_x})^{1/2}\chi^{(3)}_{\mathrm{Si}} \tag{6}$$

or

$$\chi^{(3)}_{\parallel} \approx 4\chi^{(3)}_{\mathrm{Si}} = (4 \pm 2) \times 10^{-10}\ \mathrm{esu}\ , \tag{7}$$

where we have used $\chi^{(3)}_{\mathrm{Si}} \approx 10^{-10}$ esu.

We have estimated the error bars in Eq. (7) based on the repeatability of the result from measurement to measurement. The main source of error in this determination of $\chi^{(3)}_{\parallel}$ is sample inhomogeneity (i.e., the magnitude of the reflected third-harmonic power varied somewhat from place to place on the sample and from sample to sample). This can be reduced by the development of higher quality, more uniform samples. We note again that we have used values for the complex indices of refraction taken from Kramers-Kronig analysis of reflectance data from oriented Durham *trans* polyacetylene.[8] This uncertainty can be removed by developing methods of measuring the linear-optical constants of the actual samples used.

Figure 2 displays the results of the polarization dependence of third-harmonic generation from an aligned sample. In this measurement (performed in the transmission mode), all experimental parameters were held constant, except the direction of the polarization of the incident beam. The triangles in Fig. 2 indicate the (normalized) measured power as a function of the angle between the chain direction and the polarization of the fundamental beam. When the fundamental field is polarized parallel to the chain direction, the magnitude of the third-harmonic signal is approximately 30 times larger than

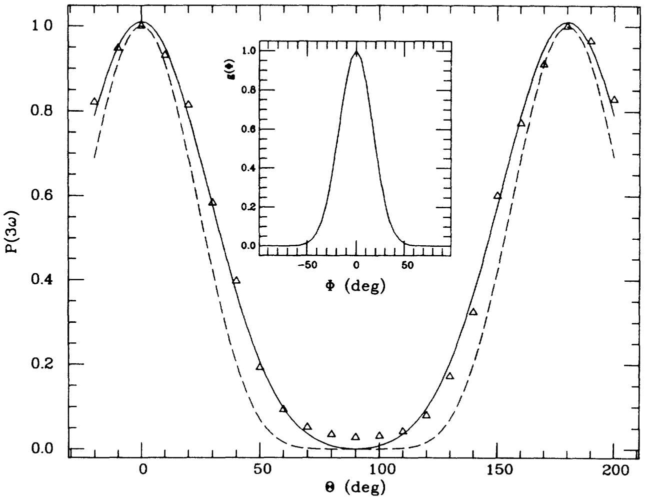

FIG. 2. Polarization dependence of third-harmonic generation from an aligned sample. The dashed curve shows the type of behavior expected for a perfectly aligned one-dimensional system ($\cos^6\theta$); the solid line represents the best fit of the functional form of Eq. (9) to the data. The best fit corresponds to a chain orientation distribution, $g(\phi)$ (as shown in the inset), with a FWHM of 40°.

when the fundamental field polarization and chain directions are orthogonal.

If we assume perfect alignment and that the only significant component of the third-order susceptibility tensor is $\chi_{\parallel}^{(3)}$, then the third-harmonic power is expected to vary as

$$P(3\omega) \propto |\chi_{\parallel}^{(3)} E_{\parallel}^{3}|^{2} \propto |\chi_{\parallel}^{(3)} \cos^{3}\theta|^{2} |E|^{6} , \quad (8)$$

where $E_{\parallel}$ is the component of the fundamental field along the chain direction, and θ is the angle between the polarization and chain directions. Note that the nonlinear polarization is parallel to $E_{\parallel}$. The dashed curve in Fig. 2 shows the type of behavior expected for a perfectly aligned one-dimensional system.

For comparison, we have measured the magnitude and the polarization dependence of the third-harmonic power from a single crystal of PDA-TS. The magnitude was obtained in a relative measurement in which the polydiacetylene third-harmonic power was directly compared to that from a *trans*-$(CH)_x$ sample (both oriented and nonoriented), which were, in turn, referenced to silicon.

The third-harmonic power reflected from the PDA-TS sample varied considerably as a function of position on the sample surface. These variations were attributed to surface roughness of the PDA polymer crystal. Since the reflection technique depends critically on surface quality, the spots yielding the highest third harmonic (and hence the best surface quality) were used. The reflected third-harmonic power was reproducible from "good" spot to "good" spot. For polyacetylene, the response was somewhat more uniform.

We found that the third-harmonic power generated on reflection from single-crystal PDA-TS was about a factor of 2 larger than that from oriented *trans*-polyacetylene. In order to complete the comparison between the nonlinear susceptibilities of these two materials, accurate values of their linear optical constants are required. If we take $N_1 \approx 2$ for PDA-TS and assume that the two materials have the same N_3, then $\chi_{\parallel}^{(3)}$ of *trans*-$(CH)_x$ is somewhat larger than that of PDA-TS. More precise measurements of these linear-optical constants are currently under way.

In evaluating the comparison between these two conjugated polymers, one must note that this measurement tends to favor PDA-TS since the "good" spots on a cleaved single-crystal surface should be of much higher surface quality than the surface of a (fibrillar) polyacetylene film. Moreover, with the incident beam at 1.06 μm (1.17 eV), the third-harmonic response of *trans*-$(CH)_x$ is at a minimum between strong resonances[3] in $\chi^{(3)}$. As a result, $\chi_{\parallel}^{(3)}$ for *trans*-$(CH)_x$ is substantially larger than that of PDA-TS for wavelengths deeper in the infrared.

The polarization dependence of the PDA-TS results are shown in Fig. 3. The third-harmonic power from the polydiacetylene crystal accurately follows the $\cos^6\theta$ relation.[14] We conclude, therefore, that is is likely that the deviations from the $\cos^6\theta$ dependence in Fig. 2 are the result of imperfect chain alignment in partially oriented *trans*$(CH)_x$ samples.

A more realistic treatment of the polarization dependence of the third-harmonic generation from the polyacetylene samples should therefore allow for some misalignment of the polymer chains. To account for this, we have fit the data to a model which incorporates a Gaussian distribution of chain orientations which is centered on the overall alignment direction. Specifically, we have assumed that the total response of the sample can be written as a sum of terms which represent chains which are oriented at an angle Φ with respect to the alignment direction, i.e.,

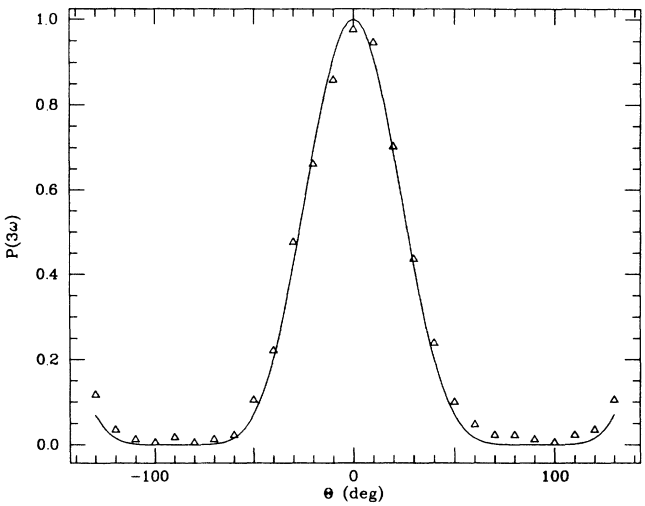

FIG. 3. Polarization dependence of the THG from PDA-TS; the third-harmonic power from the polydiacetylene crystal accurately follows the $\cos^6\theta$ relation.

$$P(3\omega) \propto \left| \int_{-\pi/2}^{\pi/2} \cos^{3}(\theta-\Phi) \exp-(\Phi/\Phi_0)^{2} d\Phi \right|^{2} , \quad (9)$$

where the width of the distribution is used as the fitting parameter. The solid line in Fig. 2 represents the best fit of the functional form of Eq. (9) to the data. The value of Φ_0 which achieves best fit corresponds to a chain distribution with FWHM of 40°, in good agreement with the value inferred from analysis of the anisotropy of the infrared absorption and from examination of electron micrographs of the fibrillar alignment.[9]

IV. SYMMETRY-SPECIFIC ORIGIN OF $\chi^{(3)}$: COMPARATIVE MEASUREMENTS OF $\chi^{(3)}$ IN *cis*- AND *trans*-POLYACETYLENE

Polyacetylene is unique in that it can be prepared in two different forms: *cis*-polyacetylene and *trans*-polyacetylene; the two isomers are shown in Fig. 4. The existence of two different isomers with different symmetry allows one to explore the specific origin of observed phenomena. *trans*-$(CH)_x$ has a twofold-degenerate ground state and can support solitons as the fundamental nonlinear excitations.[15] In *cis*-$(CH)_x$ this ground-state degeneracy has been lifted so that for the *cis* isomer the important nonlinear excitations are polarons and bipolarons. Thus, for example, subsequent to resonant (interband) photoexcitation, the shifts in oscillator strength will be quite different in the two cases. Moreover, the im-

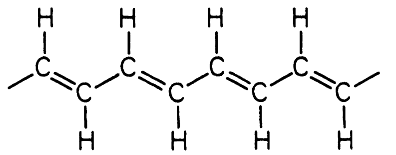

trans

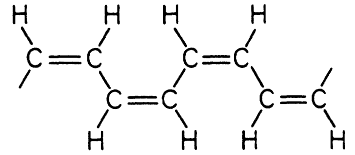

cis

FIG. 4. Chemical-structure diagrams of the two different isomers of polyacetylene.

plied changes in the nonlinear-optical properties (bigger shifts in oscillator strength imply larger $\chi^{(3)}$) due to this fundamental change in polymer symmetry can be probed on the same physical sample; conversion from *cis*- to *trans*-$(\mathrm{CH})_x$ can be accomplished simply by heating the sample to ≈150 °C for about 0.5 h.

Films of *cis*-$(\mathrm{CH})_x$ were synthesized using the Shirakawa method. By carrying out the polymerization and subsequent washing, etc. at $-78\,^{\circ}\mathrm{C}$, nearly 100% *cis*-$(\mathrm{CH})_x$ can be obtained. The *cis*-$(\mathrm{CH})_x$ samples were prepared as thick films (several micrometers in thickness) on precut glass substrates made to fit into the sample holder on the cold finger of the cryostate used for the nonlinear-optical measurements.

Since partial conversion to the *trans*-$(\mathrm{CH})_x$ isomer is unavoidable when the temperature of the polyacetylene film is raised, our initial experiments were designed to minimize the time period at room temperature. By coordinating the sample preparation with precooling of the cyrostat, we were able to reduce the room-temperature transfer time to approximately 5 min. After mounting the sample in the cryostat, the system was immediately cooled.

A precisely parallel experiment was carried out to characterize the *cis-trans* content by infrared absorption. The sample transfer time into the cryostat mounted on the Fourier-transform infrared spectrometer (FTIR) instrument was essentially identical to that required for the transfer into the THG measurement system. From the integrated intensities of the characteristic *cis*-$(\mathrm{CH})_x$ and *trans*-$(\mathrm{CH})_x$ infrared-absorption bands, we found that after transfer the polyacetylene films were approximately 15–20 % *trans*-$(\mathrm{CH})_x$.

The methodology of the initial experiment was therefore as follows: (1) Synthesis of *cis*-$(\mathrm{CH})_x$; (2) transfer of the sample into the measurement cryostate (15–20 % conversion during the transfer); (3) measurement of $P(3\omega)$ relative to the Si standard; (4) remove the polyacetylene film and isomerize at 150 °C for 0.5 h; (5) replace the same sample into the cryostat and measure $P(3\omega)$ relative to the Si standard. This process was carried out for two independently prepared samples with the same result. We found that the third-harmonic power scales with the residual *trans*-$(\mathrm{CH})_x$ content in the polyacetylene films; for a sample which is 15–20 % *trans*, the measured $\chi^{(3)}$ is approximately 15–20 % of the $\chi^{(3)}$ of the fully isomerized sample. Note that since $P(3\omega)$ is proportional to $|\chi^3|^2$, the measured third-harmonic power from the "*cis*"-$(\mathrm{CH})_x$ samples was down from that of *trans*-$(\mathrm{CH})_x$ by a factor of approximately 40. The results are consistent with negligible contribution to $P(3\omega)$ from the *cis*-$(\mathrm{CH})_x$ portion of the sample. After including the measurement uncertainties in $P(3\omega)$ and in the determination of the *cis-trans* content, we conclude that $\chi^{(3)}(\omega,\omega,\omega)$ for *cis*-$(\mathrm{CH})_x$ is at most one-tenth that of *trans*-$(\mathrm{CH})_x$.

To improve this upper limit, *cis*-$(\mathrm{CH})_x$ samples were prepared as thick (several micrometers) films in a specially constructed glass cell that allowed measurements without raising the temperature of the sample above $-78\,^{\circ}\mathrm{C}$. After completing the THG measurements on *cis*-$(\mathrm{CH})_x$, the sample was isomerized in the same cell, and the same sample was remeasured as *trans*-$(\mathrm{CH})_x$. This process was carried out for two independently prepared samples with the same result; $P(3\omega)$ from *cis*-$(\mathrm{CH})_x$ was between 250 and 500 times smaller than that from *trans*-$(\mathrm{CH})_x$, with the range due to variations in the sample surface. Since $P(3\omega)$ is proportional to $|\chi^{(3)}|^2$, the third-order susceptibility of *cis*-$(\mathrm{CH})_x$ is smaller than that of *trans*-$(\mathrm{CH})_x$ by a factor of (conservatively) 15–20.

If the mechanism for the nonlinear-optical response is related to virtual production of the nonlinear excitations of the polymer as argued in the Introduction, conversion from *cis*-$(\mathrm{CH})_x$ should have a major effect. The experimental results presented in the preceding paragraphs are consistent with this hypothesis.

V. DISCUSSION OF THE MECHANISM: $\chi^{(3)}$ FROM VIRTUAL SOLITONS ENABLED BY QUANTUM ZERO-POINT FLUCTUATIONS OF THE POLYMER CHAIN

The anisotropy of the THG for both *trans*-$(\mathrm{CH})_x$ and PDA-TS demonstrates that the nonlinearity is entirely associated with the nonlinear polarizability of the π electrons in the conjugated polymer backbone. The nearly identical magnitude of the third-harmonic response in these two materials is quite remarkable in the context of traditional explanations[16] in which the mechanism for nonlinear-optical response is nonlinear polarizability of the delocalized π electrons within a rigid lattice (and a rigid band structure). In this point of view, the third-order susceptibility would be strongly dependent on the magnitude of the single-particle energy gap (∼sixth power).[16] This is certainly not the case for the experimental results described in the preceding sections.

The onset of absorption in *trans*-$(\mathrm{CH})_x$ is well below that of PDA-TS (<1.5 eV compared with ≈2 eV). More importantly, the absorption edge at 2 eV in PDA-TS is generally accepted to be due to a neutral exciton.[17] The interband transition, as indicated by the onset of band photoconductivity[18(a)] and by electroreflectance measurements,[18(b)] is at approximately 2.4 eV. In contrast, for *trans*-$(\mathrm{CH})_x$ the onset of absorption at approximately 1.5 eV is due to an interband transition broadened on the leading edge by dynamical effects (see below) and by disorder. In *trans*-$(\mathrm{CH})_x$, the onset of photoconductivity coincides with the onset of absorption, demonstrating that there is no evidence of any bound exciton.[6] Moreover, in *trans*-$(\mathrm{CH})_x$ the signatures of photogeneration of charged solitons have the same excitation profile[19(a)] as that of the photoconductivity, and both follow the low-energy absorption tail.[19(b)] The subgap absorption below 2 eV in *trans*-$(\mathrm{CH})_x$ has been shown to be consistent with a mechanism in which the absorption tail is caused by anharmonic quantum fluctuations of the lattice.[20] In *cis*-$(\mathrm{CH})_x$, the absorption tail is suppressed relative to that of *trans*-$(\mathrm{CH})_x$, consistent with the suppression of anharmonic quantum fluctuations of the lattice due to the lifting of the ground-state degeneracy. Although the absorption edge of *cis*-$(\mathrm{CH})_x$ is close to that of PDA-TS, the third-harmonic response of the latter is at least an order of magnitude greater. Thus, the close agreement between the THG in *trans*-$(\mathrm{CH})_x$ and PDA-TS must simply be considered accidental; the nonlinear mechanisms in the two cases are different, and in neither case is the conceptually simple nonlinearity arising in third-order perturbation theory from the rigid band structure[16] the appropriate mechanism.

The data of Figs. 2 and 3 demonstrate that the nonlinear susceptibility is polarized entirely along the polymer backbone. Thus, in comparing $\chi_{\parallel}^{(3)}$ for *cis*- and *trans*-$(\mathrm{CH})_x$, one should consider the one-dimensional gaps for *intrachain* π-π^* excitation; for *cis*- and *trans*-$(\mathrm{CH})_x$, these are nearly equal. For *trans*-$(\mathrm{CH})_x$, $E_g(1\mathrm{D}) \approx 1.7$ eV has been estimated from resonant Raman scattering[21] and 1.9 eV from a fit of the absorption tail arising from anharmonic quantum fluctuations of the lattice.[20] For *cis*-$(\mathrm{CH})_x$ the 1D gap is about 2 eV. Therefore, the major difference in $\chi^{(3)}$ for the two isomers of polyacetylene appears to be larger than can be accounted for in the context of rigid-band theory [the $(E_g)^6$ dependence would predict a difference of only a factor of 2], and it implies a mechanism which is sensitive to the existence of a degenerate ground state.

In attempts directed toward a deeper understanding of the mechanisms for nonlinear-optical response of conjugated polymers, it is important to develop the connection between the *nonresonant* nonlinear response for pumping well below the absorption edge to the *resonant* nonlinear response for pumping directly into the principal absorption band. For example, in the polydiacetylene case, Greene *et al.*[22] have analyzed the resonant nonlinear response in terms of phase-space filling by one-dimensional excitons. In a beautiful argument, they showed how the concept of exciton polaritons could be used to generalize this mechanism to the nonresonant regime well below the exciton absorption edge.

For *trans*-$(\mathrm{CH})_x$, we have shown that for *resonant* pumping, the shifts in oscillator strength due to the photogeneration of charged solitons led to relatively large changes in the optical constants. In the following, we generalize this idea to the nonresonant regime where the nonlinear response is due to virtual soliton-antisoliton pairs enabled by nonlinear quantum lattice fluctuations. Following Yu, Matsuoka, and Su,[20(a)] we include fluctuations in the staggered order parameter $\phi^{n}_{n=(-1)}u_n$ which are described by the following one-parameter family of configurations [see Fig. 5(a)]:

$$\phi(x=na)=\phi_0\{1-\tanh(2x_0/\xi)[\tanh(x-x_0/\xi)-\tanh(x+x_0/\xi)]\} . \tag{10}$$

These configurations can be viewed as soliton-antisoliton pairs, where x_0 represents roughly half the separation of the soliton and antisoliton, ξ is the coherence length, and a is the lattice constant. Yu *et al.* show that within this class of configurations the total energy is of the form $E(s)=E_p(s)+(M/2)(ds/dt)^2$, where $E_p(s)$ is shown as

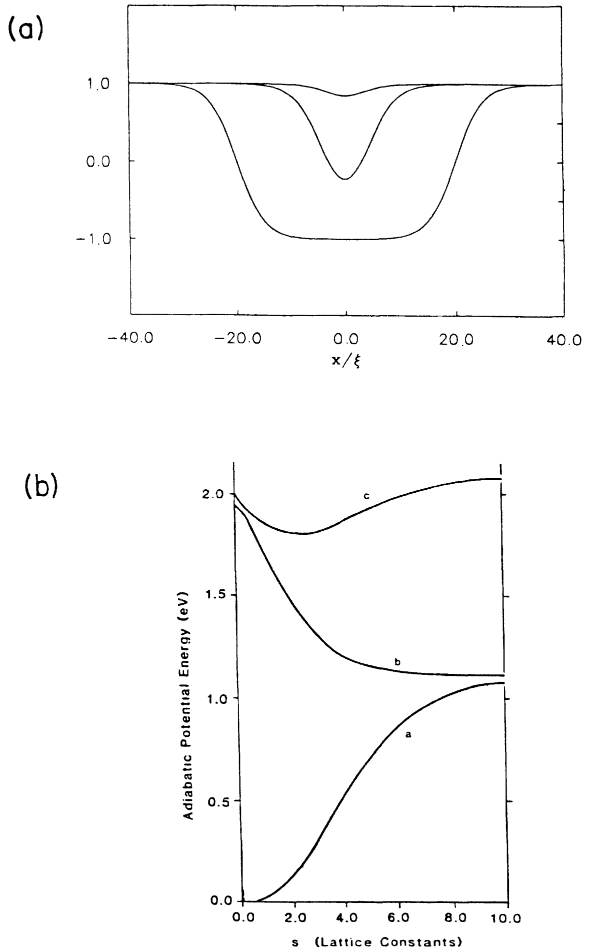

FIG. 5. (a) Sketch of the fluctuations in the staggered order parameter described by the one-parameter family of configurations: $\phi(x=na)=\phi_0\{1-\tanh(2x_0/\xi)[\tanh(x-x_0/\xi)-\tanh(x+x_0/\xi)]\}$. (b) Adiabatic potential curves for a, the electronic ground state, and b, the first- and c the second-excited states as a function of s for the configuration of (a) [from Ref. 20(a)].

curve *a* in Fig. 5(b) and s is related to x_0 by a coordinate transformation $x_0(s)$. They then treat $E_p(s)$ as an effective potential such that

$$H_0(s)=E_p(s)+(M/2)(ds/dt)^2 \tag{11}$$

is an effective Hamiltonian, and solve for the allowed bound states. They find the ground state at $E_G=0.05$ eV above the classical ground state with wave function $\phi_0(s)$ describing the nonlinear ground-state fluctuations. In addition, they have shown that there are five vibrational excited states of the s configuration, the highest one at an energy ≈ 1.8 eV above the ground state and a series of four others approximately equally spaced below 1 eV.

For each value of s there is a soliton-antisoliton pair configuration; for small s the two-gap states are close to the band edges, while for large s the two-gap states are those of widely separated solitons and appear at midgap. Thus for each s, there is a change in the absorption coefficient $\delta\alpha=(2\omega/c)\delta k$, where $n+ik$ is the complex index of refraction, $\epsilon=(n+ik)^2$. For a given s, let $\delta n_s(\omega,\omega_p)$ be the change in n at a frequency ω due to pumping a configuration s at ω_p. For example, if ω_p is above the gap, then one makes real solitons (delayed in time by $\sim 10^{-13}$ s) by the Su-Schrieffer mechanism.[23(a)] Thus for ω_p above the gap, δn_s time evolves to $\delta n_\infty(\omega)$, which comes from the shift in oscillator strength from the interband transition into the midgap transition. Since the time-resolved spectroscopy has been thoroughly studied for pumping at $\hbar\omega_p>E_g$, one knows the complete time evolution of $\delta\alpha(\omega)$ and of $\delta n(\omega)$ subsequent to pumping into the interband transition.

If the pump frequency is in the region between 2Δ and $(4/\pi)\Delta$, then one pumps the specific nonlinear configuration s of Eq. (10), which is resonant with the pump; the excited s configuration then evolves (in time) following the excited-state energy curve $E_{p'}(s)$ down (see Fig. 5) toward a well-separated charged soliton pair each with a state at midgap. Again, one expects a corresponding δn_s, which also evolves with time after the photon is absorbed from that characteristic of the originally pumped $s(t=0)$ evolving to a charged soliton pair each with state at midgap. Pumping at $\hbar\omega_p=4\Delta/\pi$ directly generates a free-soliton pair with a corresponding $\delta n_\infty(\omega)$; when pumping at the soliton-pair–creation energy there is no time delay nor any time evolution since the free-soliton pair is created directly (although with vanishingly small probability). The above are all resonant processes; they involve a real absorption of photons to form either electron-hole pairs ($\hbar\omega_p>E_g$) or excited s configurations ($\hbar\omega_p<E_g$) which time-evolve to separated charged soliton pairs. Thus, these resonant processes lead to highly nonlinear-optical phenomena with characteristic time evolution and with corresponding changes in the complex index of refraction.

What about truly virtual processes for $\hbar\omega_p$ below the $(4/\pi)\Delta$ threshold? We argue that

$$\langle\delta n(\omega,\omega_p)\rangle=\sum_s(\text{probability of finding a charged configuration } s)\delta n_s(\omega)\ .$$

Thus,

$$\langle\delta n(\omega,\omega_p)\rangle\approx\sum_s|\phi_0(s)|^2(|Q|^2/E_s)\delta n_s(\omega)\ , \tag{12}$$

where $\phi_0(s)$ is the gound-state wave function for the s configuration. The last equality holds if $\hbar\omega_p<E_s$. In Eqs. (9) and (10), $|Q|^2=e^2f_s{}^2|E|^2$ is the square of the dipole matrix element between the ground state and the (classical) electronic excited state of the s configuration at $E_{p'}(s)$; $|Q|$ is therefore proportional to the square of the oscillating electric field (i.e., the intensity of the pump) at $\omega_p<E_s$, where E_s is the appropriate energy denominator (E_s decreases from 2Δ to $4\Delta/\pi$ as s increases from 0 to ∞). Thus, from Eq. (12),

$$n(\omega)=n_0(\omega)+n_2(\omega,\omega_p)I(\omega_p)\ ,$$

[where $n_0(\omega)$ is the linear index] and from the standard phenomenology,

$$n_2(\omega,\omega_p)=(4\pi^2/c\epsilon)\chi^{(3)}(\omega,\omega_p,-\omega_p)$$

[see Eq. (2)]. Equation (12) predicts a nonlinear index (which arises directly from the nonlinear zero-point fluctuations) in response to pumping at frequencies well below the energy gap.

Note that if the ground state of the system is nondegenerate, $E_p(s)$ increases initially much more steeply with s and becomes linear for large s (soliton confinement). This suppresses the nonlinear ground-state fluctuations and suppresses the magnitude of $\langle\delta n(\omega,\omega_p)\rangle$. The predicted suppression of the nonlinear response is in agreement with our experiments comparing *cis*- and *trans*-$(\mathrm{CH})_x$.

A parallel analysis can be made of the contribution of the virtual solitons (s configurations) to the third-order nonlinearity responsible for THG. In this case, the standard third-order perturbation theory on the excited states of the s configurations yields[24]

$$\begin{aligned}\chi^{(3)}=N_0e^4\sum_{nml}(f_{gn}f_{nm}f_{ml}f_{lg})[(1/(E_{ng}-3\omega)(E_{mg}-2\omega)(E_{lg}-\omega)+1/(E_{ng}+\omega)(E_{mg}-2\omega)(E_{lg}-\omega)\\+1/(E_{ng}+\omega)(E_{mg}+2\omega)(E_{lg}-\omega)+1/(E_{ng}+\omega)(E_{mg}+2\omega)(E_{lg}+3\omega)]\ ,\end{aligned} \tag{13}$$

where $E_{ng}=(E_{s,n}-E_{s,g})$, $E_{s,g}$ is the ground-state energy, $E_{s,\alpha}$ $(\alpha=n,m,l)$ are the energies of excited states of the s configurations, $f_{\alpha\beta}$ are the dipole matrix elements. In Eq. (13), $N_0 \approx n_0\rho_c$ is the average number of soliton-antisoliton pairs on a chain of length L, and ρ_c is the density of chains per unit area. Monte Carlo simulations[25] have shown that the reduction of the dimerization order parameter due to zero-point motion is about 15%. Since this is also approximately the reduction in average order parameter in a polyacetylene ring of size 4ξ (just large enough for an $S\bar{S}$ pair), we estimate $n_0=(4\xi)^{-1}$.

In the sum, n and l denote excited states with symmetry opposite to g, and m is an excited state with the same symmetry as g. Yu, Matsuoka, and Su[20(a)] have shown that there are five vibrational excited states of the s configuration with the same parity as the ground state which contribute to $\chi^{(3)}$; one at ≈ 1.8 eV and a series of four others approximately equally spaced below 1 eV. These excited states are in product form, $\psi(s)\zeta(s)$, where $\psi(s)$ is a vibrational eigenstate and $\zeta(s)$ is the many-electron wave function associated with the classical configuration s. Thus, the matrix elements factorize into an electronic-dipole matrix element and an overlap integral, as in the usual Born-Oppenheimer approximation. *The lattice overlap integral would be zero except for the nonlinear ground-state fluctuations.*

To estimate the magnitude of $\chi^{\parallel(3)}$ we consider the term in the full sum of Eq. (13) where the matrix elements go from $g \to E_{p'}(s) \to g \to E_{p'}(s) \to g$; i.e., we ignore the various vibrational states of the s configuration and consider only this single contribution $(\chi_{\parallel}^{(3)}|_0)$

$$\chi_{\parallel}^{(3)}|_0=N_0\sum_{s,s'}|\phi_0(s)|^2|\phi_0(s')|^2(|f_s|^2|f_{s'}|^2/2\omega)[-1/(E_s-3\omega)(E_{s'}-\omega)+1/(E_s+\omega)(E_{s'}+3\omega)]\ . \tag{14}$$

For $3\omega < E_s$,

$$\chi_{\parallel}^{(3)}|_0\approx -4N_0\sum_{s,s'}|\phi_0(s)|^2\,|\phi_0(s')|^2\,|f_s|^2\,|f_{s'}|^2/E_s^2E_{s'}\ , \tag{15}$$

where f_s is the matrix element between the ground state with wave function $\phi_0(s)$ and the excited state with energy E_s relative to the ground state [see Eq. (12)]. Since

$$\alpha=N_0\sum_s|\phi_0(s)|^2\alpha_s \tag{16}$$

is the linear term in the polarizability,

$$\chi_{\parallel}^{(3)}|_0\approx-(4\alpha)\sum_s|\phi_0(s)|^2(\alpha_s/E_s)\ . \tag{17}$$

This term has a simple semiclassical origin; it arises from the modulation of the linear polarizability of the configuration s by the oscillating electric field well below resonance.

To estimate the magnitude of $\chi^{(3)}|_0$ we note that the low-frequency dielectric constant[13] of *trans*-$(\mathrm{CH})_x$ is $\epsilon_{\parallel}\sim 15$. Since the fraction of the total oscillator strength in the subgap absorption tail is approximately 20% of the total, and since that oscillator strength has an effective gap of about 1.75 eV (whereas the mean energy of the interband transition is at about 2.5 eV), we estimate $\alpha\sim\frac{1}{2}$. From Eq. (17),

$$\chi^{(3)}|_0\sim(8\xi/a)(N\rho_c)^{-1}\alpha^2/E_0\ , \tag{18}$$

where E_0 is the typical energy in the tail (~ 1.75 eV), and $N\rho_c$ is the density of carbon atoms. This is of the correct order of magnitude, i.e., $\chi_{\parallel}^{(3)}|_0\sim(1-5)\times10^{-10}$ esu. We note, furthermore, that the energies of the two- and three-photon resonances implicit in Eq. (13) are in good agreement with the resonant THG response (at 0.9 eV and for $\hbar\omega<0.5$ eV) observed by Kajzer *et al.*[3]

Detailed numerical calculations of both terms contributing to $\chi^{(3)}$ have been carried out;[2] the magnitude of the nonlinear response, the observed two-photon resonance, and the sensitivity to the lifting of the ground-state degeneracy are all in agreement with experiment.

VI. CONCLUSION

We have determined the magnitude of the third-order susceptibility associated with tripling the fundamental of the Nd:YAG laser (1.06 μm, 1.17 eV) to be $\chi_{\parallel}^{(3)}(3\omega;\omega,\omega,\omega)=(4\pm2)\times10^{-10}$ esu, where $\chi_{\parallel}^{(3)}$ refers to that component of the third-order susceptibility tensor with all indices parallel to the chain direction. By measuring anisotropic third-harmonic generation in oriented films, we have shown that this component dominates. The magnitude and anisotropy were directly compared with results obtained from single crystals of polydiacetylene-(toluene-sulfonate) measured in the same apparatus. The third-harmonic power generated by PDA-TS was found to be about a factor of 2 greater than that of *trans*-$(\mathrm{CH})_x$ (for pumping at 1.06 μm). The anisotropy of the THG for both *trans*-$(\mathrm{CH})_x$ and PDA-TS demonstrates that the nonlinear-optical properties are entirely associated with the nonlinear polarizability of the π electrons in the conjugated polymer backbone.

The close agreement between the THG in *trans*-$(\mathrm{CH})_x$ and PDA-TS was inferred to be simply accidental; the nonlinear mechanisms in the two cases are different, and in neither case is the conceptually simple nonlinearity arising from the rigid band structure in third-order perturbation theory the appropriate mechanism.

Third-harmonic generation was measured in both *cis*-rich and *trans* isomers of the same sample (before and after thermal isomerization). The measured response of the *cis*-rich samples was found to scale with the residual *trans* content, indicating that $\chi_{\parallel}^{(3)}$ of the *trans* isomer is at least an order of magnitude larger than that of the *cis* isomer.

Since $\chi^{(3)}(\omega=\omega_1+\omega_2+\omega_3)$ is a function of three independent variables, the measured $\chi^{(3)}(3\omega=\omega+\omega+\omega)$ represents a single point on a complex three-dimensional surface. The larger $\chi^{(3)}$ values implied by the resonant photoinduced absorption measurements are located in another region of this parameter space. These two regions are not unrelated, however, since one knows that the nonresonant values of the third-order susceptibility will be determined by the nature of the excited states which dominate the resonant properties.

The symmetry specific aspect of $\chi_{\parallel}^{(3)}$ is an important result and implies a mechanism which is sensitive to the existence of a degenerate ground state, as in *trans*-$(\mathrm{CH})_x$. This experimental fact is consistent with a mechanism for the third-order nonlinear-optical susceptibility of polyacetylene which involves the generation of virtual nonlinear solitons. This mechanism was explored in considerable detail, and the connection was made to the nonlinear quantum zero-point fluctuations of the polyene chain. In the absence of quantum fluctuations of the lattice, nonlinear excitations such as solitons do not affect nonresonant processes. These configurations involve lattice distortions around the photogenerated carriers; since there are no direct matrix elements between the ground state and the soliton excited states, they could only be produced by photoexcitation and subsequent decay. Inclusion of quantum flucutations allows matrix elements directly connecting the ground state and the nonlinear excited states and thereby enables virtual solitons to affect nonresonant processes. Expressions were derived for $\chi_{\parallel}^{(3)}(\omega,\omega_p,-\omega_p)$ (which leads to an intensity dependent complex index of refraction), and for $\chi_{\parallel}^{(3)}(\omega,\omega,\omega)$ (which leads to third-harmonic generation). In both cases the magnitude of the virtual soliton terms are large enough to make important contributions to $\chi_{\parallel}^{(3)}$. We conclude, therefore, that the nonlinear zero-point fluctuations of the ground state lead to an important mechanism for nonlinear-optical properties, particularly in polymers with a degenerate ground state. Lifting the ground-state degeneracy suppresses the nonlinear response, in agreement with our experimental results. In addition, the usual interband transitions, (i.e., electron-hole pairs) (Ref. 16) can be expected to influence $\chi_{\parallel}^{(3)}$. An important goal of future work will be to sort out the relative importance of the two processes in order to understand the large nonlinear susceptibility of *trans*-polyacetylene and in order to guide the development of new and better materials.

ACKNOWLEDGMENTS

We thank Dr. W.-P. Su for sending a copy of his work prior to publication and for important discussions concerning the role of solitons in $\chi^{(3)}$. We are grateful to D. McBranch for help with measurements and for comments on the proposed mechanism. We thank Professor H. Shirakawa for helping with arrangements for Dr. Akagi's visit to Santa Barbara. This research was supported by the U.S. Office of Naval Research through Contract No. N00014-86-K-0514.

---

[*] Permanent address: Institute of Material Science, University of Tsukuba, Sakura-mura, Ibaraki 305, Japan.

[†] Permanent address: Sandia National Laboratories, Albuquerque, NM 87185.

[1] (a) *Nonlinear Optical Properties of Organic and Polymeric Materials,* American Chemical Society Symposium, Series 233, edited by D. J. Williams (American Chemical Society, Washington, D.C., 1983); (b) *Nonlinear Optical Properties of Polymers,* edited by A. J. Heeger, J. Orenstein, and D. Ulrich (Materials Research Society, Pittsburgh, 1988).

[2] A. J. Heeger, D. Moses, and M. Sinclair, Synth. Met. **15**, 95 (1986).

[3] F. Kajzar, S. Etemad, G. L. Baker, and J. Messier, Synth. Met. **17**, 563 (1987); Solid State Commun. **63**, 1113 (1987).

[4] (a) J. Orenstein, in *Handbook of Conducting Polymers,* edited by T. A. Skotheim (Dekker, New York, 1986), Vol. 2; (b) A. J. Heeger, Polym. J. **17**, 201 (1985).

[5] Z. Vardeny, J. Strait, D. Moses, T.-C. Chung, and A. J. Heeger, Phys. Rev. Lett. **49**, 1657 (1982).

[6] (a) M. Sinclair, D. Moses, A. J. Heeger, K. Vilhelmsson, B. Valk, and M. Salour, Solid State Commun. **61**, 221 (1987); (b) M. Sinclair, D. Moses, and A. J. Heeger, Phys. Rev. B **36**, 4296 (1987).

[7] A. J. Heeger, D. Moses, and M. Sinclair, Synth. Met. **17**, 343 (1987).

[8] W. K. Burns and N. Bloembergen, Phys. Rev. B **4**, 3437 (1971).

[9] (a) K. Akagi, S. Katayama, H. Shirakawa, K. Araya, A. Mukoh, and T. Narahara, Synth. Met. **17**, 241 (1987); (b) K. Araya, A. Mukoh and T. Narahara, K. Akagi, H. Shirakawa, K. Araya, A. Mukoh, and T. Narahara, *ibid.* **17**, 247 (1987).

[10] M. Aldissi, J. Polym. Sci., Polym. Lett. Ed. **23**, 167 (1985).

[11] W. J. Feast, in *Handbook of Conducting Polymers,* edited by T. A. Skotheim (Dekker, New York, 1986), Vol. 1.

[12] See references listed in Ref. 8.

[13] These values were obtained from Kramers-Kronig analysis of the reflectance from highly oriented Durham polyacetylene; G. Leising (private communication).

[14] C. Sauteret, J.-P. Hermann, R. Frey, F. Pradere, J. Ducuing, R. H. Baughman, and R. R. Chance, Phys. Rev. Lett. **36**, 956 (1976).

[15] (a) S. Etemad, A. J. Heeger, and A. G. MacDiarmid, Annu. Rev. Phys. Chem. **33**, 443 (1982); (b) J. R. Schrieffer, Highlights of Condensed Matter Theory [Soc. Ital. Fis. **89**, 300 (1985)]; (c) S. Kivelson, in *Solitons,* edited by S. Trullinger and V. L. Pokrovsky (Elsevier, Amsterdam, 1986).

[16] (a) C. Flytzanis, in Ref. 1(a); (b) W. K. Wu and S. Kivelson, in Ref. 1(b), p. 229.

[17] *Polydiacetylenes* NATO Advanced Study Institute Series No. 102, edited by D. Bloor and R. R. Chance (Nijhoff, Dordrecht, 1985).

[18] (a) K. J. Donovan and E. G. Wilson, Philos. Mag. B **44**, 31 (1981); (b) L. Sebastian and G. Weiser, Chem. Physics **62**, 447 (1981).

[19] (a) G. B. Blanchet, C. R. Fincher, and A. J. Heeger, Phys. Rev. Lett. **51**, 2132 (1983); (b) B. R. Weinberger, C. B. Roxlo, S. Etemad, G. L. Baker, and J. Orenstein, Phys. Rev. Lett. **53**, 86 (1984).

[20] (a) J. Yu, H. Matsuoka, and W. P. Su, Phys. Rev. B **37**, 10 367 (1988); (b) J. P. Sethna and S. Kivelson, *ibid.* **26**, 3513 (1984); (c) A. Auerbach and S. Kivelson, *ibid.* **33**, 8171 (1986); (d) Z. B. Su and L. Yu *ibid.* **27**, 5199 (1984).

[21] Z. Vardeny, E. Ehrenfreund, O. Brafman, and B. Horovitz, Phys. Rev. Lett. **51**, 2326 (1983).

[22] B. I. Greene, J. Orenstein, R. R. Millard, and L. R. Williams, Phys. Rev. Lett. **58**, 2750 (1987).

[23] W. P. Su and J. R. Schrieffer, Proc. Natl. Acad. Sci. U.S.A. **77**, 5626 (1980).

[24] R. Loudon, *The Quantum Theory of Light* (Clarendon, Oxford, 1983).

[25] (a) W. P. Su, Solid State Commun. **42**, 497 (1982); (b) E. Fradkin and J. E. Hirsch, Phys. Rev. B **27**, 1680 (1983).

[26] M. Sinclair, D. Moses, A. J. Heeger, J. Yu, H. Matsuoka, and W. P. Su, Synth. Met. (to be published); Phys. Acta (to be published).